Dendritic Flux Avalanches and Nonlocal Electrodynamics in Thin Superconducting Films

Igor S. Aranson,[1] Alex Gurevich,[2] Marco S. Welling,[3] Rinke J. Wijngaarden,[3] Vitalii K. Vlasko-Vlasov,[1] Valerii M. Vinokur,[1] and Ulrich Welp[1]

[1]*Materials Science Division, Argonne National Laboratory, Argonne, Illinois 60439, USA*
[2]*Applied Superconductivity Center, University of Wisconsin, Madison, Wisconsin 53706, USA*
[3]*Division of Physics and Astronomy, Vrije Universiteit, 1081HV Amsterdam, The Netherlands*
(Received 15 July 2004; published 24 January 2005)

We report a mechanism of nonisothermal dendritic flux penetration in superconducting films. Our numerical and analytical analysis of coupled nonlinear Maxwell and thermal diffusion equations shows that dendritic flux pattern formation results from spontaneous branching of propagating flux filaments due to nonlocal magnetic flux diffusion and positive feedback between flux motion and Joule heating. The branching is triggered by a thermomagnetic edge instability, which causes stratification of the critical state. The resulting distribution of thermomagnetic microavalanches is not universal, because it depends on a spatial distribution of defects. Our results are in good agreement with experiments on Nb films.

Penetration of magnetic flux in a type-II superconductor can result in nonequilibrium pattern formation, such as magnetic macroturbulence [1], kinetic front roughening [2], magnetic microavalanches [3], and dendritic structures [4]. Dendritic flux penetration has been revealed by magneto-optical imaging (MOI) on multiple scales ~ 1–$100~\mu$m much greater than intervortex spacings in $YBa_2Cu_3O_7$ [5], Nb [6,7], Nb_3Sn [8], and MgB_2 [9]. Similarity of these dynamic flux patterns in different materials indicates a generic collective behavior of vortices.

It has been shown both experimentally and theoretically that dendritic flux penetration is due to a positive feedback between moving flux and the Joule heating coupled by a highly nonlinear voltage-current characteristic [4,9,10]. The resulting thermal bistability gives rise to switching waves between a cold superconducting phase and a hot resistive phase self-sustained by Joule heating [11]. Flux branching in superconductors has analogs in the theory of nonequilibrium pattern formation [12] and instability of solidification fronts [13].

Dendritic flux dynamics in superconductors was observed in numerical analysis of nonisothermal magnetic diffusion in a slab in a parallel field, when flux penetration was triggered by a local heat pulse [10]. However, experiments have been mostly done on films in a perpendicular ramping magnetic field in which case magnetic flux diffusion becomes strongly nonlocal [14]. In this Letter we calculate for the first time dynamics of dendritic flux penetration controlled by nonlocal nonlinear magnetic flux diffusion coupled to thermal diffusion in thin films. We report a novel *nonlocal* mechanism of flux branching, which captures essential features of dendritic flux penetration in superconducting films. We believe that this mechanism is generic for other nonequilibrium bistable systems exhibiting dendritic instability.

We consider a thin film strip of width w along the y axis and thickness $d \ll w$ in the xy plane perpendicular to the magnetic field H_0. Distributions of the magnetic induction, $B(\mathbf{r}, t)$, and temperature $T(\mathbf{r}, t)$ are described by the Maxwell equation coupled to heat diffusion:

$$C\partial_t T = \nabla \kappa \nabla T - (T - T_0)h/d + \mathbf{J}E(J,T), \quad (1)$$

$$\partial_t \mathbf{B} = -\nabla \times \mathbf{E}(J,T), \qquad \nabla \times \mathbf{H} = \mathbf{J}\delta(z). \quad (2)$$

Here $C(T)$ is the heat capacity, $\kappa(T)$ is the thermal conductivity, $h(T, T_0)$ is the heat transfer coefficient to the coolant or substrate held at the temperature T_0, and $\mathbf{E} = \mathbf{J}E(J,T)/J$ is the electric field, which strongly depends on $T(\mathbf{r}, t)$ and the sheet current density $\mathbf{J}(\mathbf{r}, t)$.

The $E(J, T, B)$ characteristic accounts for a resistive flux flow state with $E = (J - J_c)\rho_F$ for $J > J_c$ and a low-resistive flux creep state with $E = E_c \exp(J - J_c)/J_1$ for $J < J_c$, where $J_c(T, B)$ is the critical current density. We use the following interpolation formula expressed in terms of observable parameters [10]:

$$E = \rho_F J_1 \ln[1 + \exp(J - J_c)/J_1], \quad (3)$$

where $J_1 \ll J_c$ below the irreversibility field $B < B^*$, and $\rho_F(T) = \rho_n B/B_{c2}$ is the flux flow resistivity.

We consider weak Joule heating, for which the most essential temperature dependence comes from $E(T)$, while other parameters may be taken at $T = T_0$. The relation between current and the z component B_z in a film is given by the nonlocal Biot-Savart law. Expressing $J_x = \partial_y g$ and $J_y = -\partial_x g$ in Eq. (2) in terms of the current stream function $g(x, y, t)$, we obtain the equations for g and the dimensionless temperature θ:

$$\tau \dot{g} = \hat{K}[\partial_x[r(j,\theta)\partial_x g] + \partial_y[r(j,\theta)\partial_y g] - \tau \dot{H}_0(t)], \quad (4)$$

$$\dot{\theta} = \nabla^2 \theta - \theta + \alpha j^2 r(j, \theta). \quad (5)$$

Here we define the operator $\hat{K}$ in the Fourier space, $\hat{K} = \sum_{\mathbf{k}} \sin(k_x x)\sin(k_y y)g_{\mathbf{k}}/k$, where $k_x = \pi n/L$ and $k_y = \pi m/w$ with integers m and n ensure a zero normal component of $\mathbf{J}$ at edges of a rectangular film of width w and

length L [15]. Furthermore, $\theta = (T - T_0)/(T^* - T_0)$, $J_c(T^*) = 0$, $j = J/J_1 = [j_x^2 + j_y^2]^{1/2}$, $H_z(x, y) = \sum_{\mathbf{k}} \exp(-dk - i\mathbf{k}\mathbf{r})g_{\mathbf{k}}k/2 + H_0(t)$, the factor $\exp(-dk)$ accounts for a finite film thickness, the derivatives in Eqs. (4) and (5) are taken over normalized time t/t_h and coordinates $\mathbf{r}/L_h$, and $r(j, \theta) = \ln\{1 + \exp[j - j_c(\theta)]\}/j$ follows from Eq. (3). Here the thermal length $L_h = (d\kappa/h)^{1/2}$ and time $t_h = Cd/h$ define the spatial scale and the cooldown time of $T(\mathbf{r}, t)$ at $E = 0$. Hereafter we take $j_c(\theta) = j_0(1 - \theta)$ for $\theta < 1$, $j_c = 0$ for $\theta > 1$, and $J_1(T) = $ const [10], assume that a uniform magnetic field $H_0(t) = \dot{H}_0 t$ is ramped up with the rate $\dot{H}_0$, and neglect the field dependence of J_c. The evolution of $\theta(\mathbf{r}, t)$ and $g(\mathbf{r}, t)$ is controlled by two dimensionless parameters:

$$\tau = \frac{\mu_0\sqrt{d\kappa h}}{2\rho_F C}, \qquad \alpha = \frac{\rho J_1^2 d}{h(T^* - T_0)}. \qquad (6)$$

Here $\tau = t_m/t_h$ is the ratio of magnetic and thermal diffusion times, and α quantifies the Joule dissipation. Magnetic nonlocality strongly reduces $\tau = \tau_0 d/2L_h$ in a film as compared to $\tau_0 = \mu_0\kappa/\rho_F C$ in the bulk. Indeed, flux diffusion over a distance L_h along a film takes $t_m \sim dL_h/D_m$, while thermal diffusion takes $t_h \sim L_h^2/D_h$, where $D_m = \mu_0/\rho_F$ and $D_h = \kappa/C$. For Nb films with $d = 0.5$ μm, at 4.2 K ($\kappa \simeq 0.2$ W/cm K, $h \simeq 1$ W/cm² K, $\rho_n \simeq 3 \times 10^{-7}$ Ω cm [7], and $C \simeq 2 \times 10^{-3}$ J/cm³ K), we obtain $L_h = (d\kappa/h)^{1/2} \simeq 0.03$ mm, $t_h = Cd/h \simeq 10^{-7}$ s, $d/L_h \sim 10^{-2}$, $\tau \sim 0.1$, with τ decreasing as T_0 increases.

Using Eqs. (4) and (5) we calculated flux penetration in a film with periodic boundary conditions (bc) along x and $\partial_y \theta = g = 0$ at $y = 0, w$. Equations (4) and (5) were solved numerically by a quasispectral method based on the fast Fourier transform; up to 1024×512 harmonics were used. To implement nonperiodic bc in the y direction we used the domain of doubled length with the condition $g(x, y) = -g(x, 2w - y)$. Calculated steady-state distributions of $B_z(x)$ are very close to those of the Bean model [16]. In the majority of numerical runs for $\tau \ll 1$, we observed spontaneous avalanches induced by ramping magnetic field $H_0(t) = \dot{H}_0 t$, starting from a zero field cooled state. We also took into account randomly distributed macroscopic defects modeled by $j_c(\mathbf{r}) = j_0[1 - \theta - \sum_i q_i \cosh^{-1}(|\mathbf{r} - \mathbf{r}_i|/\xi_0)]$ where q_i, $\mathbf{r}_i$, and ξ_0 determine the strength, the position, and the radius of the ith defect. Extended current-blocking defects have been commonly revealed by the MOI [17].

Figure 1 shows flux penetration in a film with no defects (see also movie 1 in [16]). The ramping field first caused penetration of a stable cold flux front. Then an instability causing *periodic temperature modulations* and propagation of hot magnetic filaments over the preceding smooth magnetic flux distribution develops at the film edge. Once the first wave of magnetic filaments reaches the central line where the magnetization currents change direction, the filaments widen and start splitting at the ends, similar to
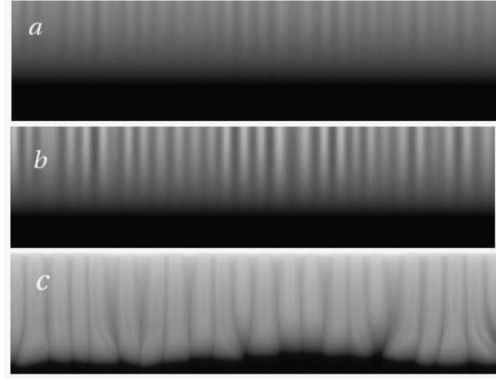

FIG. 1. Temperature distributions in a film with no defects for $\dot{H}_0 = 5J_1/t_h$, $\tau = 0.0025$, $\alpha = 0.008$, system size $600L_h \times 150L_h$ (only a quarter part is shown), and $j_0 = 20$ at (a) $t = 16.75t_h$ and (b) $t = 17.75t_h$; (c) magnetic flux pattern for $t = 20t_h$.

the flux fragmentation in a slab in a parallel field [10]. At the same time, a second wave of hot filaments start propagating from the film edge mostly between the paths of the filaments of the first wave. The new filaments are wider and exhibit shape distortions due to interaction with preceding filaments. Eventually the film cools down and the flux penetration stops, resulting in a frozen multifilamentary structure [16].

To address the mechanism of the edge instability, we performed a linear stability analysis of steady-state distributions $T(y)$ and $E_0(y)$. Because $E(J, T)$ depends on J and T, linearization of Eqs. (4) and (5) gives two coupled equations for the perturbations $\delta\theta$ and δg, which depend on $E_0(y)$ and $T(y)$. Because the flux stratification period ℓ in Fig. 1 is much smaller than the film width w while both $E_0(y)$ and $T(y)$ vary on the scale $\sim w$, we can neglect slow variations of $E_0(y)$ and $T(y)$, taking uniform $T = T_0$ and $E_0 = \dot{B}_0 w/2$ at the film edge. Then the solutions, which satisfy $\delta J_y = \partial_y \delta T = 0$ at the film edge ($y = 0$), take the form $\delta\theta \propto e^{\lambda t + ikx}\cos qy$, and $\delta g \propto e^{\lambda t + ikx}\sin qy$. From Eqs. (4) and (5), we obtain the following dispersion relation:

$$(\lambda + 1 + q^2 + k^2 - \beta)(\lambda\tau_i\sqrt{k^2 + q^2} + q^2 + sk^2) +$$
$$q^2\beta(1 + s) = 0, \qquad (7)$$

where λ and (k, q) are measured in t_h^{-1}, and L_h^{-1}, respectively. The dissipation parameter $\beta = (dJ/h)\partial E/\partial T$ depends on E_0: if $E(J) = E_c \exp[(J - J_c)/J_1]$, then $\beta \simeq E_0 J_c d|\partial J_c/\partial T|/J_1 h$ for $J < J_c$. Here $\tau_i = \mu_0\sqrt{dh\kappa}/2\rho C$ is similar to that in Eq. (6), except that ρ_F is replaced with the differential resistivity $\rho(E) = \partial E/\partial J$, and $s = E/J\rho(E) \simeq J_1/J_c$ is the flux creep rate.

Equation (7) describes coupled thermal and magnetic diffusion modes, the factor $\sqrt{k^2 + q^2}$ accounting for the magnetic nonlocality. Positive eigenvalues $\lambda(k, q)$ correspond to unstable modes resulting in spontaneous thermo-

magnetic structures similar to those for a slab in a parallel field [18]. For slow flux diffusion $\tau \gg 1$, thermal perturbations with $\lambda \simeq \beta - 1 - k^2 - q^2$ are unstable above the thermal runaway threshold, $\beta > 1$. In this case λ is maximum at $k = q = 0$ so no periodic structures are expected. A completely different situation occurs for fast flux diffusion $\tau \ll 1$ for which Eq. (7) yields

$$\lambda = \beta - 1 - q^2 - k^2 - \frac{q^2 \beta(1+s)}{q^2 + sk^2}. \quad (8)$$

The spectrum of q is determined by the full set of boundary conditions in the theory of flux jumps [19]. For further qualitative analysis we take $q \simeq \pi/2b$, where $\delta J_x(x, b) = 0$, $b = [1 - 1/\cosh(B_0/B_p)]w/2$ is the width of the flux penetrated critical state region, and $B_p = \mu_0 J_c/\pi$ [20]. For a given q, the increment $\lambda(q, k)$ passes through a maximum at the wave vector k_m, which defines the period $\ell = 2\pi/k_m$ of the fastest growing thermomagnetic structure along the film. Here $sk_m^2 = [q^2 \beta s(1+s)]^{1/2} - q^2$, thus $\lambda(k, q)$ is maximum at the finite k_m if $\beta > \beta_i = q^2/s(1+s)$ or $\dot{B}_0 > \dot{B}_i$. For $s \ll 1$, we obtain $\dot{B}_i$ and ℓ in normal units:

$$\dot{B}_i = \frac{\pi^2 \kappa}{4b^3|\partial J_c/\partial T|}, \qquad \ell^2 = \frac{16b^2 s}{(\dot{B}_0/\dot{B}_i)^{1/2} - 1}. \quad (9)$$

Here ℓ decreases as $1/s$ and $\dot{B}_0$ increase, in agreement with our numerical results [16]. The short-wave instability with $k_m > 0$ and $\mathrm{Re}\,\lambda(\beta_c, k_m, q) > 0$ occurs at $\beta = \beta_c$ in Eq. (8); that is, $\dot{B}_0 > \dot{B}_c = hJ_1\beta_c/dbJ_c|\partial J_c/\partial T|$, where

$$\beta_c^{1/2} = (1 + 2q^2)^{1/2} + q\sqrt{1 + 1/s}. \quad (10)$$

For $\tau_i \ll 1$, Eq. (10) gives $\beta_c > \beta_i$ for all $q(t) = \pi/2b(t)$, so a thermomagnetic structure with the finite period $\ell(\beta_c) \ll b$ develops as the width $b(t)$ exceeds b_c, where $\dot{B}_0 = \dot{B}_c(b_c)$. Equation (7) defines a region $\tau_1 < \tau < \tau_2$ in which λ is complex, which manifests itself in temporal oscillations of growing flux structures.

Next we consider dendritic flux penetration initiated by macroscopic defects, both at the film edge and in the bulk. Such defects can trigger local flux jumps even if the critical state in the bulk is stable [21] and cause branching instability of flux filaments in a slab in a parallel field [10]. Figure 2 shows selected flux patterns in a film where edge defects produce flux fingers superimposed with a smooth flux front. This behavior is characteristic of any superconductor with a highly nonlinear $E(J)$, for which a defect of size ξ_0 produces a much larger disturbance $\simeq \xi_0/s$ across the current flow [22]. The flux fingers widen and split at the ends as they collide with the central line where magnetization currents change direction [10]. As j_0 increases, hot flux filaments in Figs. 2(b) and 2(c) get thinner and start branching even *before* they reach the central line. Then new fingers start growing between the defects due to the edge instability considered above; see animations for more details [16]. Moreover, in wider samples [Figs. 2(c) and
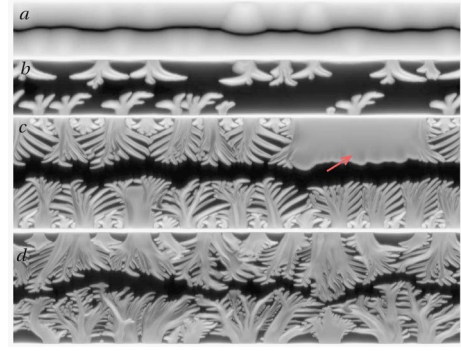

FIG. 2 (color online).   Flux penetration in a film of $320L_h \times 40L_h$ with 30 random edge defects with $\xi_0 = 0.25L_h$, and amplitudes q_i uniformly distributed between 0 and 0.4, for $\dot{H}_0 = 3J_1/t_h$, $\alpha = 0.08$, $\tau = 0.0025$, and $t = 25t_h$ for (a) $j_0 = 20$ and (b) $j_0 = 80$. Black and white correspond to the Meissner and vortex phases, respectively. (c) Wide film of $600L_h \times 150L_h$ with 20 edge defects for $\dot{H}_0 = 5J_1/t_h$, $j_0 = 60$. The giant avalanche develops in a defect free region marked by the arrow. (d) Same wide film with 500 randomly distributed bulk defects at $j_0 = 80$. See also movies 2–6 in [16].

2(d)] the finger undergoes multiple branching, giving rise to the characteristic flux dendrites. This new branching mechanism, which was not observed in simulations of flux patterns in a slab [10], is due to nonlocal flux diffusion in films. Thinning of the filaments as s decreases follows from Eq. (9), while the branching instability is facilitated by magnetic nonlocality, which causes a weaker damping of short-wave electromagnetic modes $\lambda_m \propto k$ as compared to local flux diffusion for which $\lambda_m \propto k^2$. Another new effect at higher j_0 is a "giant" flux avalanche in Fig. 2(c), which starts propagating from the region with no surface defects after the first wave of smaller flux filaments reached the center.

Figure 2(d) shows flux patterns in a film with randomly distributed bulk defects. In addition to the branching due to magnetic nonlocality, propagating flux filaments can undergo splitting caused by local transient heat spikes as they collide with defects. This results in local shape instability of the filaments and their subsequent branching similar to that obtained for local magnetic flux diffusion [10]. With the decrease of j_0 (which is equivalent to an increase of T_0 or H_0 in the experiment) flux filaments become wider and eventually start overlapping, forming a continuous flux front. However, even in this case a significant front roughness still persists both due to a size distribution of individual filaments and due to local heat releases as the flux front collides with defects [16].

The dendritic flux penetration can be regarded as *avalanches* of vortex bundles which do not trigger a global flux jump in the whole sample. Such avalanches produce local temperature spikes, partial flux penetration, and a step on magnetization curves $M(B)$ [3,4]. Nonlocal electrodynamics of films strongly facilitates branching flux propagation, which requires faster magnetic diffusion
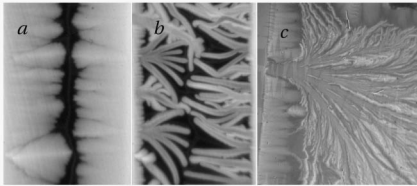
FIG. 3.   MOI of flux branching in Nb films of Ref. [7] at
(a) $T = 6.2$ K and $B_0 = 31.2$ mT and (b) $T = 4.7$ K and $B_0 = 36.5$ mT. (c) "Giant flux avalanche" at 4.5 K in the Nb film of
[23]. See also movies 7–8 in [16].

$\tau = \tau_0 \sqrt{dh/\kappa} \ll 1$ characteristic of thin films with $dh \ll \kappa$. Notice that because $b \sim w(B_0/B_p)^2$ for small B_0, both
critical ramp rates $\dot{B}_i \propto B_0^{-6}$ and $\dot{B}_c \propto B_0^{-6}$ strongly depend
on the applied field B_0 for $B_0 \ll B_p$ but level off for $B_0 > B_p$ as $b \rightarrow w/2$. Furthermore, both $\dot{B}_i$ and $\dot{B}_c$ increase as
T_0 increases. Thus, for a given $\dot{B}_0$, the branching occurs at
lower T above a certain field $B_i(T)$, in agreement with
many experiments [5–9].

Figure 3 shows MOI of flux penetration in two different
Nb films in ramping fields. One 9 mm $\times$ 1.8 mm $\times$
0.5 μm Nb film described in detail elsewhere [7] exhibits
flux patterns similar to those in Figs. 2(a) and 2(b) where
dendritic flux penetration is initiated by surface defects.
For this film ($\kappa = 0.2$ W/cm K and $h = 1$ W/cm^2 K),
we obtain $dh/\kappa \sim 10^{-4}$ and the thermal length $L_h = (d\kappa/h)^{1/2} = 0.03$ mm, much smaller than the film width
$w = 1.8$ mm (i.e., the film width is about $60L_h$ as in
Figs. 2(a) and 2(b)], in which case the magnetic nonlocality
does play the key role. Figure 3(c) shows MOI of an
effectively wider (4 mm $\times$ 4 mm $\times$ 0.1 μm) film [23]
($w \sim 10^2 L_h$), in which in addition to small microava-
lanches near the film edge a giant avalanche, similar to
that triggered by a laser pulse in YBa$_2$Cu$_3$O$_7$ [5] and those
in Figs. 2(c) and 2(d), develops.

In conclusion, we proposed a mechanism of flux frag-
mentation caused by coupling of nonlocal flux diffusion
with local thermal diffusion. The nonlocality results in the
following effects: (1) It strongly reduces the parameter τ,
facilitating the periodic short-wave instability as a precur-
sor of flux branching. (2) It reduces damping of short-wave
electromagnetic perturbations, making it easier for den-
dritic flux patterns to develop. (3) It accelerates magnetic
flux propagation, which may explain the superfast flux
propagation observed in films [5]. (4) It causes coexistence
of multiscale dendrites and giant flux avalanches induced
by surface and bulk defects.

[1] V. K. Vlasko-Vlasov *et al.*, Physica (Amsterdam) **222C**,
361 (1994); M. R. Koblishka *et al.*, Europhys. Lett. **41**,
419 (1998).
[2] R. Surdeanu *et al.*, Phys. Rev. Lett. **83**, 2054 (1999).
[3] S. Field *et al.*, Phys. Rev. Lett. **74**, 1206 (1995); E. R.
Nowak *et al.*, Phys. Rev. B **55**, 11 702 (1997).
[4] E. Altshuler and T. H. Johansen, Rev. Mod. Phys. **76**, 471
(2004).
[5] P. Leiderer *et al.*, Phys. Rev. Lett. **71**, 2646 (1993);
U. Bolz *et al.*, Europhys. Lett. **64**, 517 (2003); Physica
(Amsterdam) **388C**, 715 (2003).
[6] C. A. Duran *et al.*, Phys. Rev. B **52**, 75 (1995).
[7] M. S. Welling *et al.*, Physica (Amsterdam) **406C**, 100
(2004).
[8] I. A. Rudnev *et al.*, Cryogenics **43**, 663 (2003).
[9] M. Baziljevich *et al.*, Physica (Amsterdam) **369C**, 93
(2002); T. H. Johansen *et al.*, Europhys. Lett. **59**, 599
(2002); F. L. Barkov *et al.*, Phys. Rev. B **67**, 064513
(2003).
[10] I. Aranson, A. Gurevich, and V. Vinokur, Phys. Rev. Lett.
87, 067003 (2001).
[11] A. V. Gurevich and R. G. Mints, Rev. Mod. Phys. **59**, 941
(1987).
[12] M. C. Cross and P. C. Hohenberg, Rev. Mod. Phys. **65**, 851
(1992).
[13] J. S. Langer, Rev. Mod. Phys. **52**, 1 (1980).
[14] E. H. Brandt, Rep. Prog. Phys. **58**, 1465 (1995); A.
Gurevich, Int. J. Mod. Phys. B **9**, 1045 (1995).
[15] Because scales of our flux structures are much smaller that
the film width, we used a large-*k* asymptotics of the kernel
$\hat{K}$ in the general equation for $g(\mathbf{r}, t)$ by E. H. Brandt, Phys.
Rev. B **52**, 15 442 (1995).
[16] See EPAPS Document No. E-PRLTAO-94-002506 for an
extensive collection of movies of dendritic flux and tem-
perature patterns. A direct link to this document may be
found in the online article's HTML reference section. The
document may also be reached via the EPAPS homepage
(http://www.aip.org/pubservs/epaps.html) or from ftp.ai-
p.org in the directory /epaps/. See the EPAPS homepage
for more information.
[17] V. K. Vlasko-Vlasov, G. W. Crabtree, U. Welp, and V. I.
Nikitenko, in *Physics and Materials Science of Vortex
States, Flux Pinning and Dynamics*, NATO Advanced
Study Institutes, Ser. E, Vol. 356 (Kluwer, Dordrecht,
1999), p. 205; D. Larbalestier, A. Gurevich, D. M.
Feldman, and A. Polyanskii, Nature (London) **414**, 368
(2001); Ch. Jooss *et al.*, Rep. Prog. Phys. **65**, 651 (2002).
[18] A. L. Rakhmanov *et al.*, Phys. Rev. B **70**, 224502 (2004).
[19] R. G. Mints and A. L. Rakhmanov, Rev. Mod. Phys. **53**,
551 (1981).
[20] E. H. Brandt and M. V. Indenbom, Phys. Rev. B **48**, 12 893
(1994); E. Zeldov *et al.*, *ibid.* **49**, 9802 (1994).
[21] R. G. Mints and E. H. Brandt, Phys. Rev. B **54**, 12 421
(1996); A. Gurevich, Appl. Phys. Lett. **78**, 1891 (2001).
[22] A. Gurevich and M. Friesen, Phys. Rev. B **62**, 4004
(2000).
[23] V. K. Vlasko-Vlasov *et al.*, Phys. Rev. B **69**, 140504
(2004).